



HOKKAIDO UNIVERSITY

Title	Substitution of Deoxycholate with the Amphiphilic Polymer Amphipol A8-35 Improves the Stability of Large Protein Complexes during Native Electrophoresis
Author(s)	Kameo, Shinsa; Aso, Michiki; Furukawa, Ryo et al.
Citation	Plant and Cell Physiology, 62(2), 348-355 https://doi.org/10.1093/pcp/pcaa165
Issue Date	2021-01-05
Doc URL	https://hdl.handle.net/2115/85167
Rights	This is a pre-copyedited, author-produced version of an article accepted for publication in Plant and cell physiology following peer review. The version of record is available online at: https://academic.oup.com/pcp/article/62/2/348/6064163 , https://doi.org/10.1093/pcp/pcaa165 .
Type	journal article
File Information	Plant and Cell Physiology62(2)_348-355.pdf



1 **This is a “clear copy” of the revised manuscript. The content is exactly the same as**
2 **“marked copy” described above.**

3

4 **Cover page**

5

6 **Title:** Substitution of deoxycholate with the amphiphilic polymer amphipol A8-35
7 improves the stability of large protein complexes during native electrophoresis

8

9 **Running Title:** Improved Stability with Clear Native-PAGE

10

11 **Corresponding Author:** Atsushi Takabayashi

12 Institute of Low Temperature Science, Hokkaido University, N19 W8 Kita-Ku, Sapporo

13 060-0819, Japan

14 E-mail: takabayashi@pop.lowtem.hokudai.ac.jp

15 Tel: +81-75-706-5493; Fax: +81-75-706-5493

16

17 **Subject Area:** (11) new methodology

18 **Number of black and white figures: 0**

19 **Number of color figures:** 6

20 **Number of tables:** 0

21 **Type and number of supplementary materials:** 3 figures

22 **Title: Substitution of deoxycholate with the amphiphilic polymer amphilipol A8-35**
23 **improves the stability of large protein complexes during native electrophoresis**

24

25 **Running Title:** Improved Stability with Clear Native-PAGE

26

27 Shinsa Kameo¹, Michiki Aso¹, Ryo Furukawa¹, Renon Matsumae¹, Makio Yokono²,

28 Tomomichi Fujita³, Ayumi Tanaka¹, Ryouichi Tanaka¹, Atsushi Takabayashi¹

29 ¹Institute of Low Temperature Science, Hokkaido University, N19 W8 Kita-ku,

30 Sapporo 060-0819, Japan

31 ²Innovation Center, Nippon Flour Mills Co., Ltd., Atsugi 243-0041, Japan

32 ³Faculty of Science, Hokkaido University, N10 W8 Kita-ku, Sapporo 060-0810, Japan

33

34 **Abbreviations:** BN, blue-native; CBB, Coomassie brilliant blue; CN, clear-native; α -

35 DDM, α -dodecyl maltoside; DOC, sodium deoxycholate; LHC, light-harvesting

36 complex; polyacrylamide gel electrophoresis (PAGE)

37

38 **Abstract**

39 Native polyacrylamide gel electrophoresis (PAGE) is a powerful technique for protein
40 complex separation that retains both their activity and structure. In photosynthetic
41 research, native-PAGE is particularly useful given that photosynthetic complexes are
42 generally large in size, ranging from 200 kD to 1 MD or more. Recently, it has been
43 reported that the addition of amphipol A8-35 to solubilized protein samples improved
44 protein complex stability. In a previous study, we found that amphipol A8-35 could
45 substitute sodium deoxycholate (DOC), a conventional electrophoretic carrier, in clear-
46 native (CN)-PAGE. In this study, we present the optimization of amphipol-based CN-
47 PAGE. We found that the ratio of amphipol A8-35 to α -dodecyl maltoside (α -DDM), a
48 detergent commonly used to solubilize photosynthetic complexes, was critical for
49 resolving photosynthetic machinery in CN-PAGE. In addition, LHCII dissociation from
50 PSII-LHCII was effectively prevented by amphipol-based CN-PAGE compared with
51 that of DOC-based CN-PAGE. Our data strongly suggest that majority of the PSII-
52 LHCII *in vivo* forms $C_2S_2M_2$ at least in *Arabidopsis* and *Physcomitrella*. The other
53 forms might appear owing to the dissociation of LHCII from PSII during sample
54 preparation and electrophoresis, which could be prevented by the addition of amphipol
55 A8-35 after solubilization from thylakoid membranes. These results suggest that

56 amphipol-based CN-PAGE may be a better alternative to DOC-based CN-PAGE for the
57 study of labile protein complexes.

58

59 **[Introduction]**

60 Oxygenic photosynthetic organisms possess two photosystems, PSI and PSII,
61 which are comprised of core and peripheral antenna complexes. The core antenna
62 complex harvests light energy and transfers it to the reaction center where charge
63 separation and the first electron transfer step occur. In comparison, the peripheral light-
64 harvesting antenna associated with the PSII core harvests light energy and transfers the
65 excitation energy to the core complex, where charge separation and the first electron
66 transfer step occurs. Heat dissipation of the excess energy primarily occurs in the
67 peripheral antenna complex. The core complexes of both PSI and PSII are highly
68 conserved among photosynthetic organisms, while peripheral antenna systems are quite
69 diverse (Blankenship 2010; Croce and van Amerongen 2014; Neilson and Durnford
70 2010; Nelson and Junge 2015). The diversity of the peripheral antenna system should be
71 key to the adaptation of photosynthetic organisms to a wide range of environments.

72 The peripheral antenna complexes of green plants, including green algae and
73 land plants, are comprised of light-harvesting complexes (LHCs). Light harvesting

74 complex proteins bind chlorophyll *a*, chlorophyll *b*, and carotenoids, which are
75 indispensable for multiple LHC antenna functions. The LHCs can be associated with
76 PSI and PSII to form PS supercomplexes (Caffarri et al. 2014; Gao et al. 2018; Kouril et
77 al. 2012; Pan et al. 2019). Notably, the number of LHCs associated with PSI and PSII
78 can be dynamically changed in response to environmental changes (Pan et al. 2019).
79 Dynamic structural changes in the size of the peripheral antenna of photosystems may
80 reveal the adaptive mechanisms of photosynthetic species.

81 Blue-Native (BN)-PAGE is a powerful technique that can be used to resolve
82 protein complexes. For the analysis of photosynthetic complexes from various
83 photosynthetic organisms, BN-PAGE has been used to separate the components of the
84 thylakoid membranes that are solubilized with mild detergents such as dodecyl
85 maltoside (α -DDM) or digitonin (Järvi et al. 2011; Wittig et al. 2006). Since BN-PAGE
86 allows for the native structure and activity of protein complexes to be retained during
87 electrophoresis, broad downstream BN-PAGE applications have been reported, such as
88 proteomic identification, pigment composition evaluations, spectroscopic analyses, and
89 the reconstitution of protein structures using electron microscopy (Wittig et al. 2006).
90 As such, multiple post-BN-PAGE applications have furthered the analysis of
91 photosynthetic machinery from various perspectives.

92 Coomassie brilliant blue (CBB) dye is used in BN-PAGE to negatively charge
93 protein complexes, which enables them to be resolved at neutral pH (Wittig et al. 2006).
94 The presence of CBB on the protein surface reduces the dissociation risk due to protein-
95 protein interactions when detergents are present (Wittig et al. 2006). However, the blue
96 color of the CBB dye inhibits some downstream experiments, including absorption
97 spectra measurements of the resolved photosynthetic complexes. In addition, CBB dye
98 can act as a competitive quencher of chlorophyll fluorescence in LHCII (Yokono,
99 2015). In such cases, CBB is substituted with sodium deoxycholate (DOC), a colorless
100 compound that negatively charges proteins. This form of PAGE is referred to as clear
101 native (CN)-PAGE (Järvi et al. 2011; Wittig and Schägger 2005). However, the use of
102 DOC as an electrophoresis carrier may promote dissociation due to protein-protein
103 interactions, which is not a problem when CBB is used (Witting and Schägger 2005).
104 Thus, an alternative to DOC in CN-PAGE is needed.

105 Amphipols are a new class of amphipathic polymers that enable membrane
106 protein complexes to be solubilized while enhancing their stability in detergent-free
107 solutions (Popot et al. 2011). In particular, amphipol A8-35 has been widely used to
108 stabilize membrane proteins (Popot et al. 2011). In addition, a pioneering study with

109 *Chlamydomonas* showed that amphipol A8-35 was able to stabilize PSII-LHCII
110 supercomplexes during sucrose density gradient centrifugation (Watanabe et al. 2019).

111 In addition to its stabilizing effect on membrane proteins, amphipol A8-35 can
112 negatively charge protein complexes under conditions of neutral pH due to its
113 negatively charged surface. These characteristics suggest that amphipol A8-35 may be a
114 good alternative to DOC. We recently tested the ability of an amphipol-based CN-PAGE
115 to resolve photosynthetic protein complexes with *Physcomitrella* (Furukawa et al.
116 2019). In the current study, we demonstrated that the substitution of DOC with
117 amphipol A8-35 improved the stability of the photosynthetic machinery, especially for
118 the PSII-LHCII supercomplexes during CN-PAGE separation. The resolution of
119 amphipol-based CN-PAGE was comparable to that of DOC-based CN-PAGE. Our
120 results strongly suggest that amphipol-based CN-PAGE is a better alternative to DOC-
121 based CN-PAGE with the potential for a wide variety of downstream applications.

122

123 **[Results]**

124 **Optimization of the ratio of amphipol A8-35 to α -DDM on CN-PAGE**

125 The first step of amphipol-based CN-PAGE is the addition of amphipol A8-35
126 instead of DOC to maintain the solubility of the protein complex. Owing to the slow

127 dissociation of amphipols from membrane proteins (Popot et al. 2011), the addition of
128 amphipol A8-35 to the cathode buffer is not necessary during electrophoresis (Furukawa
129 et al. 2019). Since amphipol A8-35 is much more expensive than DOC, it is also cost-
130 effective to avoid the addition of amphipol A8-35 to the cathode buffer. However, no
131 optimization of the A8-35: α -DDM ratio for a given protein sample has yet to be
132 reported.

133 To optimize the A8-35: α -DDM ratio, we evaluated the changes in *Arabidopsis*
134 photosynthetic machinery band patterns as the amphipol A8-35 concentration varied.
135 The concentration of α -DDM was fixed at 1% to solubilize *Arabidopsis* thylakoid
136 protein complexes. After electrophoresis, several pigment-protein complexes were
137 observed, including the PSII-LHCII supercomplexes, PSI-LHCI and LHCII (Fig. 1).
138 Band identification was conducted using 2D-SDS-PAGE with silver staining (Fig. S1)
139 according to the band patterns of previous studies (i.e., Järvi et al. 2011; Takabayashi et
140 al. 2011). Although the band patterns were very similar between 1% and 0.5% amphipol
141 A8-35, slight differences were observed. Specifically, the mobility of PSI-LHCI and
142 LHCII trimers showed greater impairment with 0.5% amphipol A8-35 than with 1%
143 amphipol A8-35 (Fig. 1). This impaired mobility suggests that the quantity of amphipol
144 A8-35 bound to the photosynthetic machinery was not saturated when 0.5% amphipol

145 A8-35 was employed. However, when the amphipol A8-35 concentration was lower
146 than 0.25%, apparent differences were present among the band patterns. Specifically,
147 the LHCII trimers and PSI-LHCI bands were poorly resolved. These results demonstrate
148 that amphipol A8-35: α -DDM ratio in a given sample is important for resolving protein
149 complexes by amphipol-based CN-PAGE.

150 Since surfactants and amphipols competitively bind to the protein surface
151 (Popot et al. 2011), a low amphipol A8-35: α -DDM ratio may inhibit the binding of
152 amphipol A8-35 to the surface of the protein. To evaluate this hypothesis, we reviewed
153 changes in the band patterns as the α -DDM concentration increased from 1-4% while
154 the amphipol A8-35 concentration was fixed at 1%. As expected, the resolution
155 worsened as the α -DDM concentration increased (Fig. 2). Finally, we reviewed band
156 patterns as the α -DDM concentration increased with a fixed amphipol A8-35: α -DDM
157 ratio. When the ratio of amphipol A8-35 to α -DDM was fixed, the band patterns
158 presented little variability, even when the α -DDM concentration increased from 1 to 4%
159 (Fig. 3). These results indicated that amphipol A8-35: α -DDM ratio was important for
160 ensuring sufficient resolution when amphipol A8-35 was not added to the cathode
161 buffer. It is noteworthy that the separation pattern of the photosynthetic complexes in
162 amphipol-based CN-PAGE did not significantly worsen even when high concentration

163 α -DDM (4%) was used for solubilization (Fig. 3). This strongly suggests that the
164 dissociation of LHCII from PSII by high concentration α -DDM occurs extensively
165 during electrophoresis, which can be prevented by the addition of amphipol A8-35 after
166 solubilization.

167

168 **Optimization of the timing of adding amphipol A8-35 to a solubilized protein** 169 **sample**

170 In a previous study, amphipol A8-35 was added to solubilized protein samples
171 after centrifugation. In this study, we optimized the timing of amphipol A8-35 addition
172 to protein samples. It should be noted that although α -DDM is a mild detergent, it
173 promotes the dissociation of LHCII from PSI-LHC and PSII-LHCII (Järvi et al. 2011).
174 Thus, we hypothesized that the early addition of amphipol A8-35 to a protein sample
175 would reduce the risk of LHCII dissociation.

176 We noted that the photosystems were hardly solubilized by α -DDM when
177 amphipol A8-35 was included in the thylakoid membrane solution. Similarly, the
178 amounts of solubilized photosystems were greatly reduced when A8-35 was added
179 immediately after mixing the samples with α -DDM (Fig. 4a). However, a two minute
180 incubation period, after mixing the thylakoid sample with α -DDM prior to the addition

181 of A8-35, resulted in a considerable amount of solubilized photosystem as when A8-35
182 was added after centrifugation (Fig. 4b). These data strongly suggest that amphipol A8-
183 35 inhibits the solubilization of the membrane protein complexes in thylakoids by α -
184 DDM, unless there is enough incubation time before adding A8-35 to the sample. In
185 addition, we found that the band patterns were similar regardless of whether amphipol
186 A8-35 was added to the protein samples either before or after centrifugation (Fig. 4).
187 These results suggest that LHCII dissociation rarely occurred during the short 5-min
188 centrifugation (Fig. 4).

189

190 **Comparison of the band patterns of *Arabidopsis* and *Physcomitrella* thylakoid**
191 **protein complexes between DOC-based CN-PAGE and amphipol-based CN-PAGE**
192 **using amphipol A8-35**

193 To compare amphipol-based CN-PAGE using amphipol A8-35 with DOC-
194 based CN-PAGE, we resolved α -DDM-solubilized *Arabidopsis* thylakoid protein
195 complexes using the two methods (Fig. 5). The identification of the resolved bands by
196 DOC-based CN-PAGE was performed by 2D-SDS-PAGE followed by silver staining
197 (Fig. S1), following the methodology of Furukawa et al. (2019). We found that the PSI-
198 LHCI, LHCII trimer, LHC monomers, and free pigments were well resolved by both

199 methods (Fig. 5). Since free pigments appeared yellow in color, they likely contained
200 more carotenoids than chlorophylls. On the other hand, we found notable differences in
201 the resolution of the PSII-LHCII supercomplexes (Fig. 5). The three PSII-LHCII forms
202 were observed with DOC-based CN-PAGE. The largest PSII-LHCII form was $C_2S_2M_2$.
203 As the number of attached LHCII decreases, the $C_2S_2M_2$ form changes to C_2S_2M and
204 then to C_2S_2 (Caffarri et al. 2009; Pan et al. 2019; Su et al. 2017; van Bezouwen et al.
205 2017; Wei et al. 2016). The most commonly observed PSII-LHCII forms in both
206 methods were $C_2S_2M_2$ and C_2S_2M . In addition, the band intensity of $C_2S_2M_2$ seemed
207 more prominent than that of C_2S_2M on amphipol-based CN-PAGE. In contrast, the C_2S_2
208 band was clearly observed in DOC-based CN-PAGE, whereas this band was hardly
209 observed in amphipol-based CN-PAGE. The greater quantity of C_2S_2 in DOC-based
210 CN-PAGE compared to that of amphipol-based CN-PAGE was likely owing to the
211 dissociation of LHCII from the larger PSII-LHCII forms. These results strongly suggest
212 that LHCII detachment from PSII-LHCII was low when amphipol A8-35 was employed
213 with CN-PAGE.

214 The same trend was observed for CN-PAGE with *Physcomitrella* thylakoid
215 protein complexes. A PSII-PSI megacomplex, PSII-LHCII supercomplexes, PSI-LHCI,
216 LHCII trimer, and LHCII monomer were resolved (Fig. 6). To identify the resolved

217 bands, we performed 2D-CN/SDS-PAGE followed by silver staining (Fig. S2).

218 Although the overall band patterns were similar between DOC-based CN-PAGE and

219 amphipol-based CN-PAGE, a notable difference was observed between these methods

220 (Fig. 6). Two PSII-LHCII bands were clearly observed with DOC-based CN-PAGE,

221 whereas one PSII-LHCII band was clearly observed with amphipol-based CN-PAGE.

222 The additional PSII-LHCII band found in the DOC-based CN-PAGE had a lower

223 molecular weight, which suggests that LHCII partially dissociated from PSII-LHCII.

224 The low molecular weight form of PSII-LHCII may have possibly been C₂S₂M.

225 However, the PSII-LHCII supercomplex forms in *Physcomitrella* have not yet been

226 fully elucidated. Therefore, we were unable to identify the low molecular weight form

227 of PSII-LHCII as C₂S₂M in this study. These results indicated that amphipol A8-35 was

228 superior to DOC when preventing LHCII dissociation from PSII-LHCII in CN-PAGE.

229 Furthermore, these data strongly suggest that majority of the PSII-LHCII *in vivo* forms

230 C₂S₂M₂ in *Arabidopsis* and *Physcomitrella*. The other forms of PSII-LHCII are likely to

231 have emerged as a result of the dissociation of LHCII from PSII during sample

232 preparation and electrophoresis.

233

234 **[Discussion]**

235 **The ratio of amphipol A8-35 to α -DDM in a sample is important to resolve**

236 **membrane protein complexes**

237 In this study, we optimized amphipol-based CN-PAGE protocols. Since amphipol A8-35
238 is negatively charged, amphipol A8-35-bound membrane protein complexes can migrate
239 during electrophoresis at neutral pH. On the other hand, CBB and DOC must be added
240 to the cathode buffer for BN-PAGE and DOC-based CN-PAGE, respectively. This
241 difference is based on the chemical properties of amphipol A8-35. Amphipol A8-35
242 tightly and noncovalently binds to the hydrophobic surfaces of membrane protein
243 complexes and shows an extremely slow dissociation rate (Popot et al. 2011). Owing to
244 this property, amphipol A8-35 was not added to the cathode buffer during
245 electrophoresis. However, amphipol A8-35 dissociates from membrane proteins in the
246 presence of competing surfactants, such as α -DDM. This is likely the reason why using
247 a proper amphipol A8-35: α -DDM ratio is important to achieve good protein complex
248 resolution (Figs 1-3).

249 If a sufficient amount of amphipol A8-35 is added to the cathode buffer, the
250 amphipol A8-35: α -DDM ratio in the loading sample may not be important. However,
251 the economic cost of amphipol-based CN-PAGE is much higher when using amphipol
252 A8-35 in the cathode buffer.

253

254 **Amphipol A8-35 can efficiently prevent the dissociation of LHCII from PSII-**
255 **LHCII supercomplexes during CN-PAGE**

256 We found that the amphipol-based CN-PAGE method was better able to separate PSII-
257 LHCII supercomplexes while retaining their intact forms than the CN-PAGE method
258 when using *Arabidopsis* and *Physcomitrella* thylakoid membranes (Fig. 5 and 6).

259 Specifically, greater dissociation of LHCII from the PSII-LHCII supercomplexes
260 seemed to occur both with *Arabidopsis* and *Physcomitrella* when using DOC-based CN-
261 PAGE. These results are consistent with those of a previous report in which amphipol
262 A8-35 was found to prevent the dissociation of LHCII from the PSII-LHCII
263 supercomplexes with *C. reinhardtii* during sucrose density gradient separation
264 (Watanabe et al. 2019). It is noteworthy that membrane protein complexes are typically
265 much more stable with amphipols compared to their stability in detergent solutions
266 (Popot et al. 2011). Thus, amphipol A8-35-PSII-LHCII complexes in detergent-free
267 states are likely to be more stable than PSII-LHCII complexes in α -DDM solutions or
268 DOC solutions. As such, amphipol-based-CN-PAGE facilitates the retention of intact
269 PSII-LHCII forms during sample preparation and electrophoresis.

270 Our findings that the C₂S₂ M₂ was the major form of the PSII-LHCII on
271 amphipol-based CN-PAGE (Figs 5 and S1) strongly suggest that PSII-LHCII should be
272 essentially a C₂M₂S₂ *in vivo*, and other forms are likely to emerge owing to the
273 dissociation of LHCII from PSII during the experimental procedure. Accordingly,
274 amphipol-based CN-PAGE can be a useful tool to reveal the dynamics of the PSII-
275 LHCII supercomplexes in response to environmental changes.

276

277 **Potential applications of amphipol-based CN-PAGE**

278 Previous reports have shown that amphipols typically enhance protein stability but do
279 not interfere with protein function (Popot et al. 2011). These properties permit a wide
280 variety of applications using amphipols, including protein structural and functional
281 analyses. In addition, BN-PAGE and DOC-based CN-PAGE can separate protein
282 complexes while retaining their structure and function, allowing for a wide variety of
283 downstream applications using these methods (Wittig et al. 2006; Wittig and Schagger
284 2005). Specifically, BN-PAGE and CN-PAGE have often been used to separate
285 membrane protein complexes with mild detergents, including α -DDM and digitonin.
286 Here, we found that amphipol-based CN-PAGE can be applied to separate membrane
287 protein complexes solubilized by α -DDM and digitonin (Fig. S3). It is noteworthy that

288 digitonin is the only known detergent that can retain the PSI-LHCI-LHCII complex
289 after solubilization (Järvi et al. 2011). Due to these advantages, amphipol-based CN-
290 PAGE is likely to have wide-ranging applications. In particular, the advantage of CN-
291 PAGE over BN-PAGE is that CBB does not interfere with spectroscopic and pigment
292 analyses. Since these analyses are important for understanding photosystem properties,
293 CN-PAGE with amphipol A8-35 is preferable to BN-PAGE. In addition, given the
294 stabilizing effect of amphipol A8-35, structural and functional analyses following
295 amphipol-based CN-PAGE may yield better results than those of either DOC-based BN-
296 or CN-PAGE. Nonetheless, further studies are needed to verify the potential of
297 amphipol-based CN-PAGE.

298

299 **[Materials and Methods]**

300 **Plants and growth conditions**

301 *Arabidopsis thaliana* ecotype Columbia plants were grown in soil for 6 weeks at 23°C
302 with a 14:10 h (light:dark) photoperiod that employed 70 $\mu\text{mol photons m}^{-2} \text{s}^{-1}$.

303 Protonemata from *Physcomitrella patens* were cultured for 4 days on a layer of
304 cellophane overlaid on BCDAT (BCD medium supplemented with 1 mM CaCl_2 and
305 5 mM di-ammonium [+-]tartrate) that was solidified with 0.8% (w/v) agar at 25°C under

306 continuous light conditions ($40 \mu\text{mol photons m}^{-2} \text{s}^{-1}$), following the methodology of
307 Furukawa et al. (2019).

308

309 **Separation of thylakoid protein complexes by CN-PAGE**

310 *Arabidopsis* thylakoid membrane isolation followed the methodology of Järvi et al.
311 (2011). *Physcomitrella* thylakoid membrane isolation was performed according to the
312 methodology of Furukawa et al. (2019). Unless otherwise noted, the thylakoid
313 membranes were solubilized with 1% α -DDM in a solubilization buffer (50 mM
314 imidazole/HCl, pH 7.0, 20% glycerol) with 10 mM sodium fluoride and a protease
315 inhibitor cocktail for plant cell lysate (Sigma, St. Louis, MO, USA) at 4°C and
316 centrifuged at $22,500 \times g$ for 5 min at 4°C.

317 For amphipol-based CN-PAGE, amphipol A8-35 was added to the supernatants
318 at a final concentration of 1%. The supernatants with amphipol A8-35 were separated on
319 4-13% polyacrylamide gradient gels at 4°C using anode (50 mM imidazole/HCl, pH
320 7.0, 4°C) and cathode buffers (50 mM Tricine and 15 mM imidazole/HCl, pH 7.0, 4°C),
321 according to the methodology of Furukawa et al. (2019). Amphipol A8-35 was not
322 added to the cathode buffer of amphipol-based CN-PAGE. For DOC-based CN-PAGE,
323 0.05% DOC and 0.02% α -DDM were added to the cathode buffer following the

324 methodology of Järvi et al. (2011). Native Mark Unstained Protein Standard (Thermo
325 Fisher Scientific, Rockford, IL, USA) was used as a marker of molecular size.

326

327 **2D-SDS-PAGE followed by immunoblot analysis and silver staining**

328 Proteins in the CN-PAGE gel strip were denatured in a solubilization buffer (1% SDS
329 and 50 mM DTT) for 30 min at 25°C and separated on a 14% acrylamide gel containing
330 4 M urea using the Laemmli system following the methodology of Furukawa et al.
331 (2019). Silver staining was performed using the Pierce Silver Stain kit (Thermo Fisher
332 Scientific, Rockford, IL, USA), according to the manufacturer's protocol. Precision
333 Plus Protein All Blue Standards (Bio-Rad, Hercules, CA, USA) was used as a marker of
334 molecular size. The separated proteins were transferred to a PolyScreen polyvinylidene
335 fluoride membrane (PerkinElmer Life Sciences, MA, USA). The PsaD, PsbB, and
336 Lhcb2 subunits were detected using specific antibodies and a Western Lightning Plus-
337 ECL kit (PerkinElmer Life Sciences). All antibodies, including anti-PsaD (AS09 461),
338 anti-PsbB (AS04 038), and anti-Lhcb2 (AS01 003) were purchased from Agrisera
339 (Vännäs, Sweden).

340

341 **[Funding]**

342 This work was supported by a Grant-in-Aid for Scientific Research from the Japan
343 Society for the Promotion of Science [grant number: 17K07691 to A. Takabayashi and
344 grant number: 16H06554 to R. Tanaka].

345

346 **[Disclosures]**

347 Conflicts of interest: The authors declare no conflicts of interest.

348

349 **[References]**

350 Blankenship, R.E. (2010) Early Evolution of Photosynthesis. *Plant Physiol.* 154: 434-
351 438.

352

353 Caffarri, S., Kouril, R., Kereiche, S., Boekema, E.J. and Croce, R. (2009) Functional
354 architecture of higher plant photosystem II supercomplexes. *EMBO J.* 28: 3052-3063.

355

356 Caffarri, S., Tibiletti, T., Jennings, R.C. and Santabarbara, S. (2014) A comparison
357 between plant photosystem I and photosystem II architecture and functioning. *Curr.*
358 *Protein Pept. Sc.* 15: 296-331.

359

360 Croce, R. and van Amerongen, H. (2014) Natural strategies for photosynthetic light
361 harvesting. *Nat. Chem. Biol.* 10: 492-501.

362

363 Furukawa, R., Aso, M., Fujita, T., Akimoto, S., Tanaka, R., Tanaka, A., et al. (2019)
364 Formation of a PSI-PSII megacomplex containing LHCSR and PsbS in the moss
365 *Physcomitrella patens*. *J. Plant Res.* 132: 867-880.

366

367 Gao, J.L., Wang, H., Yuan, Q.P. and Feng, Y. (2018) Structure and Function of the
368 Photosystem Supercomplexes. *Front. Plant Sci.* 9.

369

370 Järvi, S., Suorsa, M., Paakkarinen, V. and Aro, E.M. (2011) Optimized native gel
371 systems for separation of thylakoid protein complexes: novel super- and mega-
372 complexes. *Biochem. J.* 439: 207-214.
373

374 Kouril, R., Dekker, J.P. and Boekema, E.J. (2012) Supramolecular organization of
375 photosystem II in green plants. *Biochim. Biophys. Acta Bioenerg.* 1817: 2-12.
376

377 Neilson, J.A.D. and Durnford, D.G. (2010) Structural and functional diversification of
378 the light-harvesting complexes in photosynthetic eukaryotes. *Photosynth. Res.* 106: 57-
379 71.
380

381 Nelson, N. and Junge, W. (2015) Structure and energy transfer in photosystems of
382 oxygenic photosynthesis. *Annu. Rev. Biochem.* 84: 659-683.
383

384 Pan, X., Cao, P., Su, X., Liu, Z. and Li, M. (2019) Structural analysis and comparison of
385 light-harvesting complexes I and II. *Biochim. Biophys. Acta Bioenerg* 148038.
386

387 Popot, J.L., Althoff, T., Bagnard, D., Baneres, J.L., Bazzacco, P., Billon-Denis, E., et al.
388 (2011) Amphipols From A to Z. *Annu. Rev. Biophys.* 40: 379-408.
389

390 Su, X.D., Ma, J., Wei, X.P., Cao, P., Zhu, D.J., Chang, W.R., et al. (2017) Structure and
391 assembly mechanism of plant C₂S₂M₂-type PSII-LHCII supercomplex. *Science* 357:
392 815-820.
393

394 Takabayashi, A., Kurihara, K., Kuwano, M., Kasahara, Y., Tanaka, R. and Tanaka, A.
395 (2011) The oligomeric states of the photosystems and the light-harvesting complexes in
396 the Chl *b*-less mutant. *Plant Cell Physiol.* 52: 2103-2114.
397

398 van Bezouwen, L.S., Caffarri, S., Kale, R.S., Kouril, R., Thunnissen, A.M.W.H.,
399 Oostergetel, G.T., et al. (2017) Subunit and chlorophyll organization of the plant
400 photosystem II supercomplex. *Nat. Plants* 3.
401

402 Watanabe, A., Kim, E., Burton-Smith, R.N., Tokutsu, R. and Minagawa, J. (2019)
403 Amphipol-assisted purification method for the highly active and stable photosystem II
404 supercomplex of *Chlamydomonas reinhardtii*. *FEBS Lett.* 593: 1072-1079.
405

406 Wei, X.P., Su, X.D., Cao, P., Liu, X.Y., Chang, W.R., Li, M., et al. (2016) Structure of
407 spinach photosystem II-LHCII supercomplex at 3.2 angstrom resolution. *Nature* 534:
408 69-74.

409

410 Wittig, I., Braun, H.P. and Schägger, H. (2006) Blue native PAGE. *Nat. Protoc.* 1: 418-
411 428.

412

413 Wittig, I. and Schägger, H. (2005) Advantages and limitations of clear-native PAGE.
414 *Proteomics* 5: 4338-4346.

415

416

417 **[Figure legends]**

418 **Fig. 1 Changes in the band pattern of amphipol-based CN-PAGE with amphipol**

419 **A8-35.** *Arabidopsis* thylakoid protein complexes were solubilized by 1% α -DDM. After
420 centrifugation, amphipol A8-35 was added to the supernatants for final concentrations
421 of 1%, 0.5%, 0.25%, and 0.125%. The samples were separated by 4-13% acrylamide
422 gels. No amphipol A8-35 was added to the cathode buffer.

423

424 **Fig. 2 Changes in the band pattern of amphipol-based CN-PAGE as the**

425 **concentration of α -DDM varied.** *Arabidopsis* thylakoid protein complexes were
426 solubilized by 1%, 2%, and 4% α -DDM. After solubilization, amphipol A8-35 was
427 added to the supernatants at a final concentration of 1%. The samples were loaded and
428 separated by 4-13% acrylamide gels. No amphipol A8-35 was added to the cathode
429 buffer.

430

431 **Fig. 3 The changes in the band pattern of the amphipol-based CN-PAGE with the**
432 **same ratio of amphipol A8-35 to α -DDM.** *Arabidopsis* thylakoid protein complexes
433 were solubilized by 1%, 2%, and 4% α -DDM. After solubilization, amphipol A8-35 was
434 added to the supernatants for final concentrations of 1%, 2%, and 4%, respectively. The
435 ratio of amphipol A8-35 to α -DDM was the same among the samples. The samples were
436 loaded and separated by 4-13% acrylamide gels. No amphipol A8-35 was added to the
437 cathode buffer.

438

439 **Fig. 4 Band patterns of amphipol-based CN-PAGE when amphipol A8-35 was**
440 **added to the samples either before or after centrifugation.** *Arabidopsis* thylakoid
441 protein complexes were solubilized by 1% α -DDM. (a) Immediately after mixing the
442 samples with α -DDM, amphipol A8-35 was added to the supernatants either before or
443 after centrifugation. (b) After mixing with α -DDM and the subsequent incubation for 2
444 min, amphipol A8-35 was added to the supernatants either before or after centrifugation.
445 The samples were loaded into and separated by 4-13% acrylamide gels. No amphipol
446 A8-35 was added to the cathode buffer.

447

448 **Fig. 5 *Arabidopsis* thylakoid protein complexes resolved by DOC-based and**
449 **amphipol-based CN-PAGE.** *Arabidopsis* thylakoid protein complexes were solubilized
450 by 1% α -DDM and resolved by the DOC-based (A) and amphipol-based (B) CN-PAGE.
451 After solubilization, amphipol A8-35 was added to the supernatants at a final
452 concentration of 1% (B). The samples were loaded and separated by 4-13% acrylamide
453 gels. The cathode buffer of the DOC-based CN-PAGE contained 0.05% DOC and
454 0.02% α -DDM. No amphipol A8-35 was added to the cathode buffer for amphipol-
455 based CN-PAGE.

456

457 **Fig. 6 *Physcomitrella* thylakoid protein complexes resolved by amphipol-based and**
458 **DOC-based CN-PAGE.** *Physcomitrella* thylakoid protein complexes were solubilized
459 by 1% DDM and resolved by and amphipol-based (A) and DOC-based (B) CN-PAGE.
460 After solubilization, amphipol A8-35 was added to the supernatants at a final
461 concentration of 1% (A). The samples were loaded and separated by 4-13% acrylamide
462 gels. The cathode buffer of the DOC-based CN-PAGE contained 0.05% DOC and
463 0.02% α -DDM. No amphipol A8-35 was added to the cathode buffer for amphipol-
464 based CN-PAGE.

Fig. 1

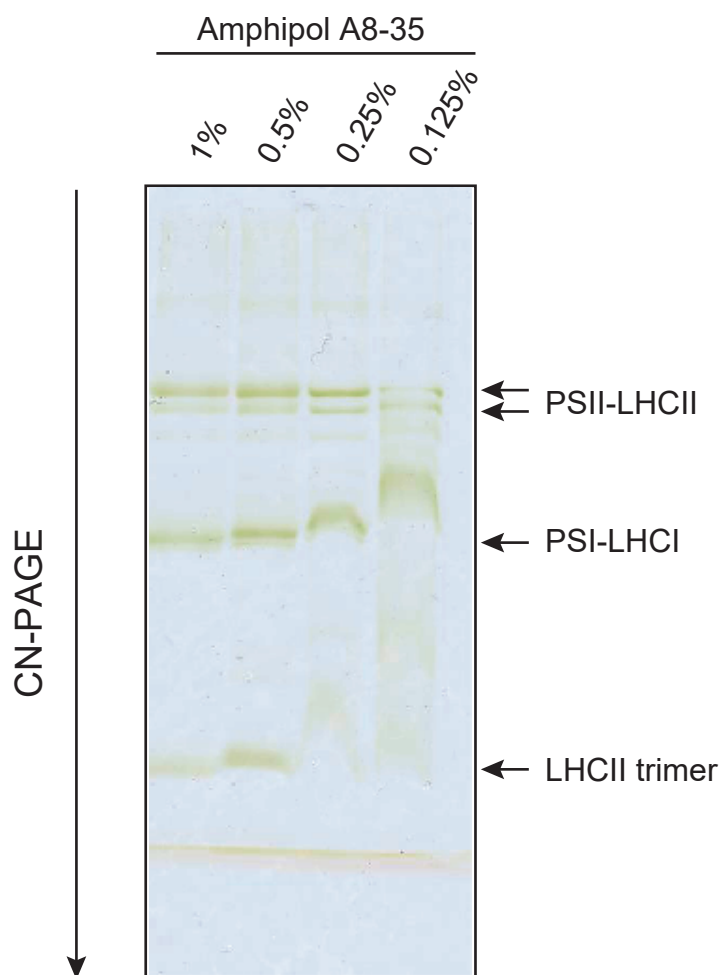


Fig. 2

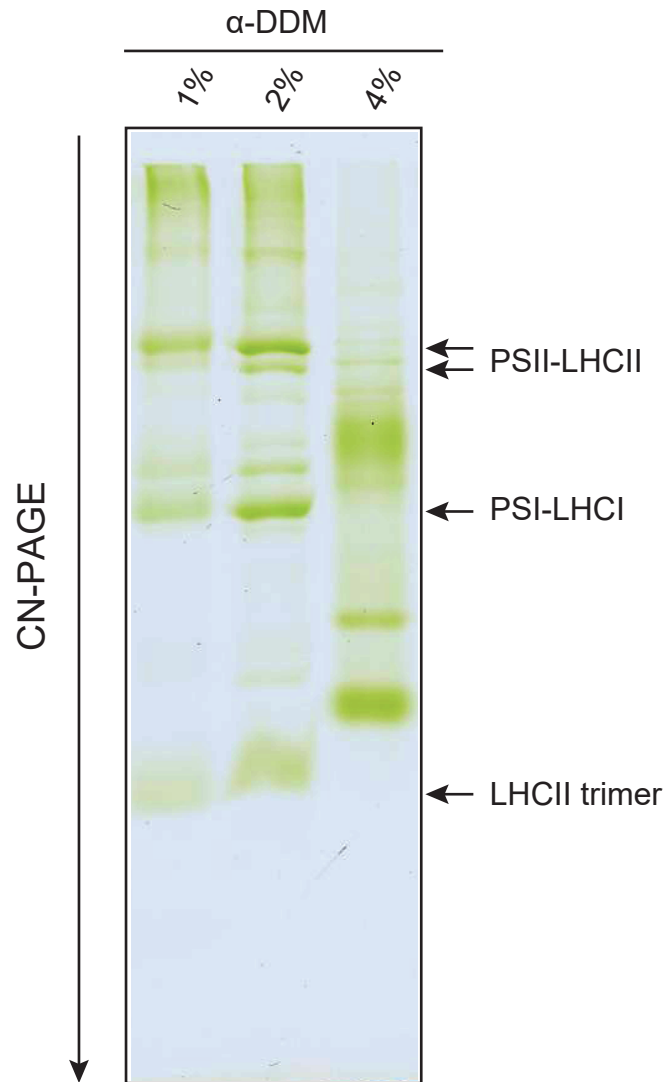


Fig. 3

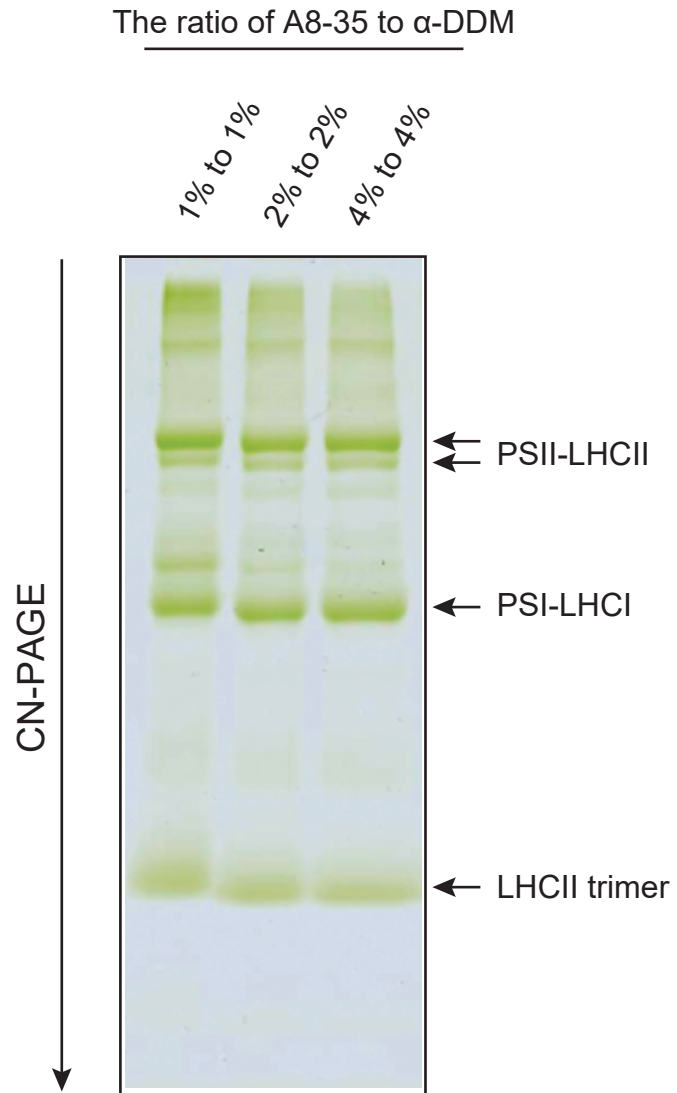


Fig. 4

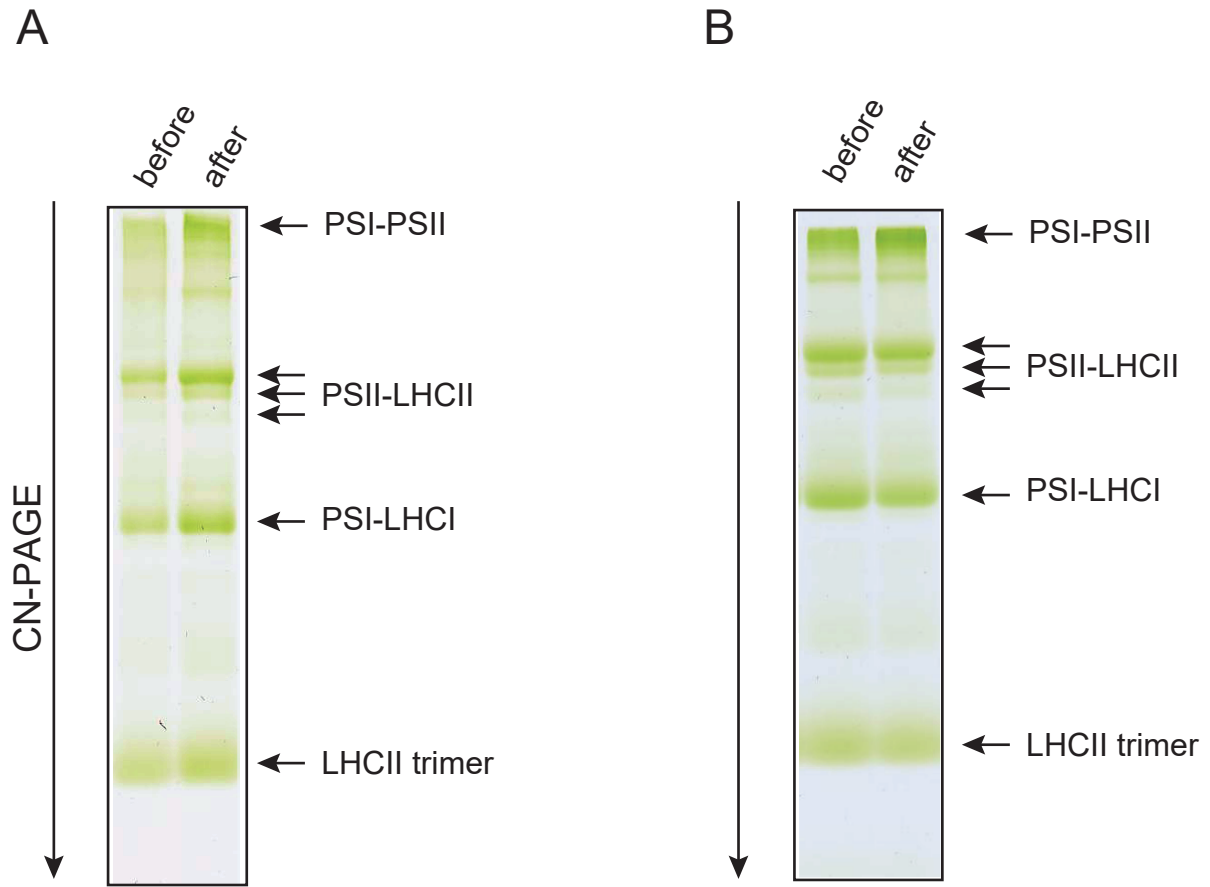


Fig. 5

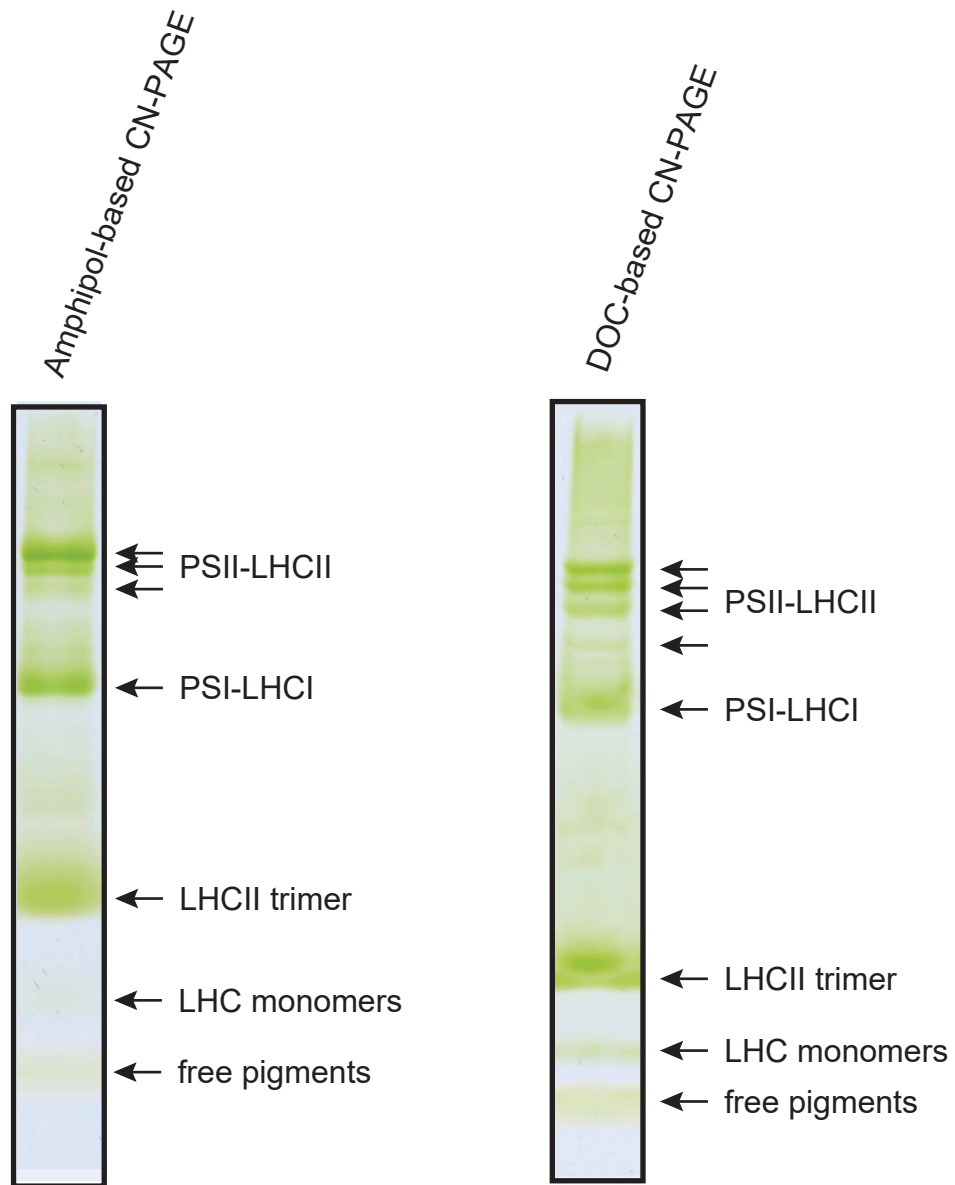
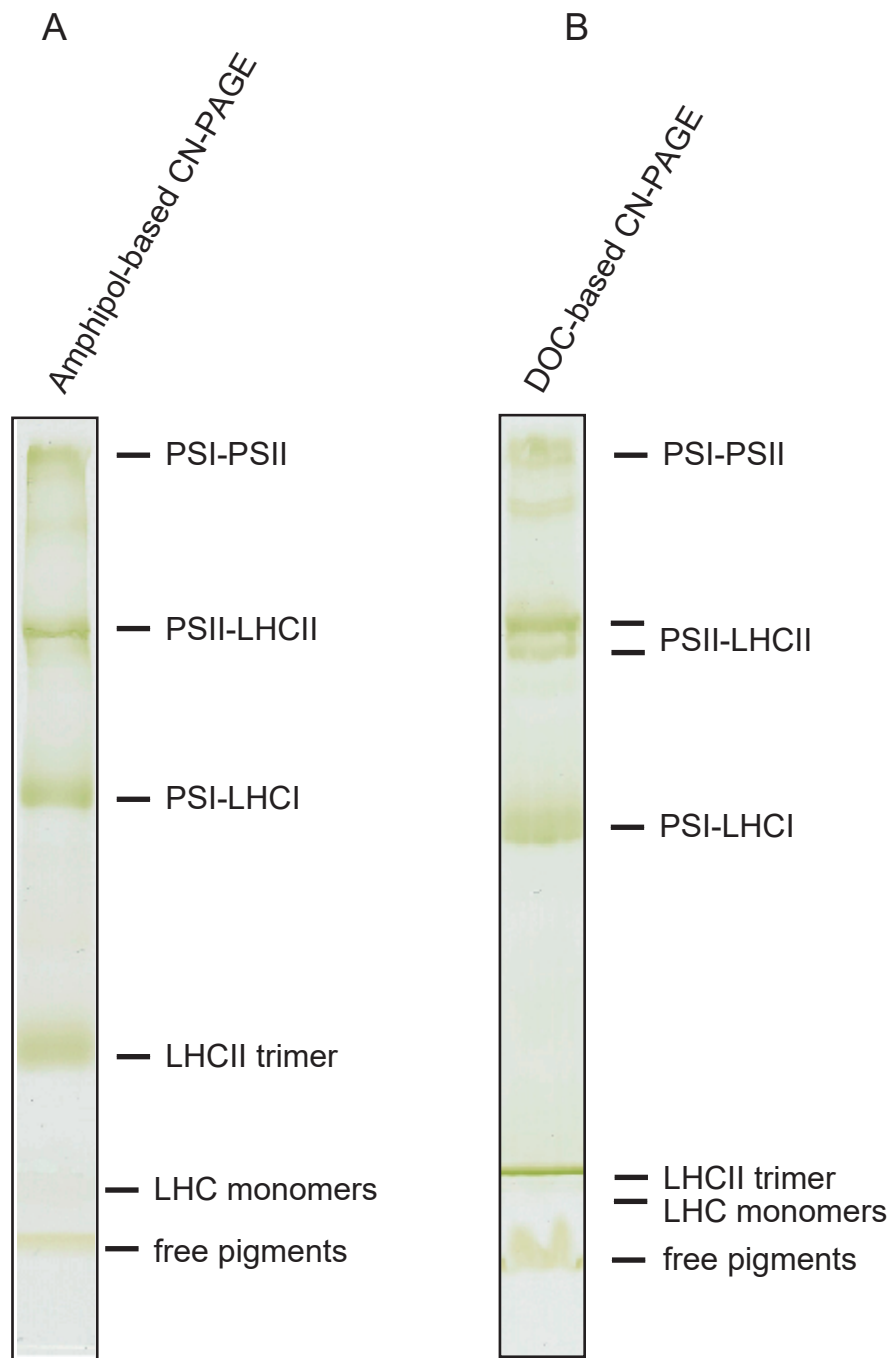
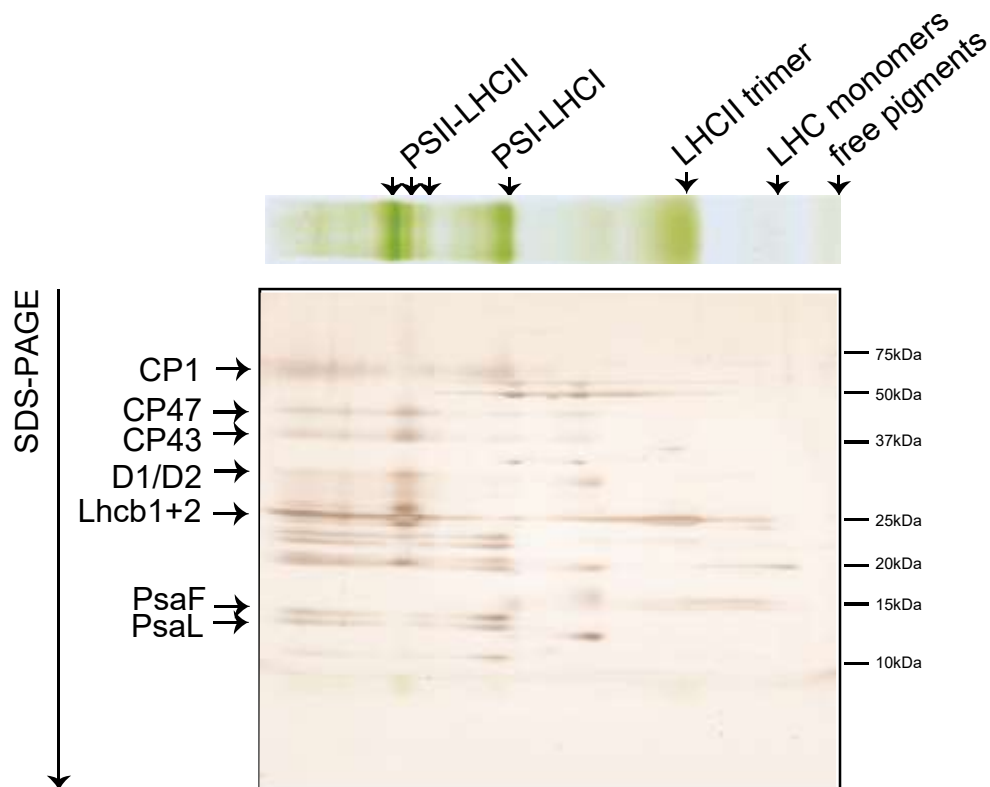


Fig. 6



A



B

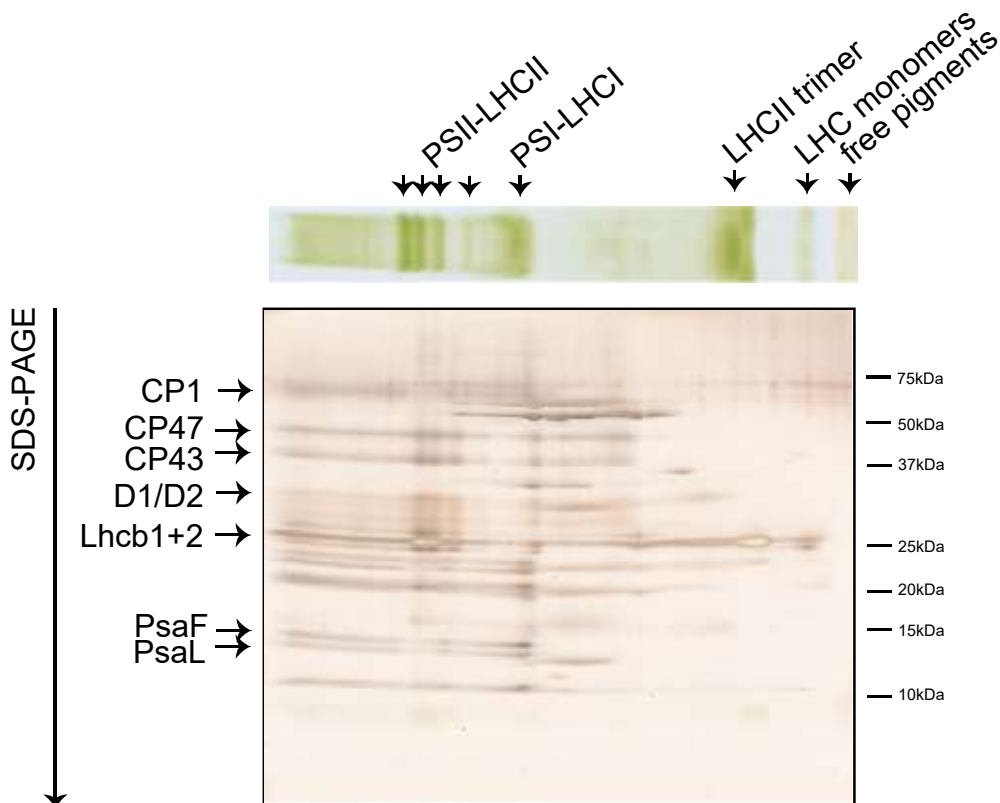


Fig. S1 2D-CN/SDS-PAGE of *Arabidopsis* protein complexes in thylakoid membranes followed by silver staining. The amphipol-based (a) and DOC-based (b) CN-PAGE gel strips (Fig. 5) were soaked in 1% SDS and 50 mM DTT solution for 30 min. Proteins in the gel strips were resolved by SDS-PAGE using a 14% acrylamide gel containing 6 M urea and visualized by silver staining.

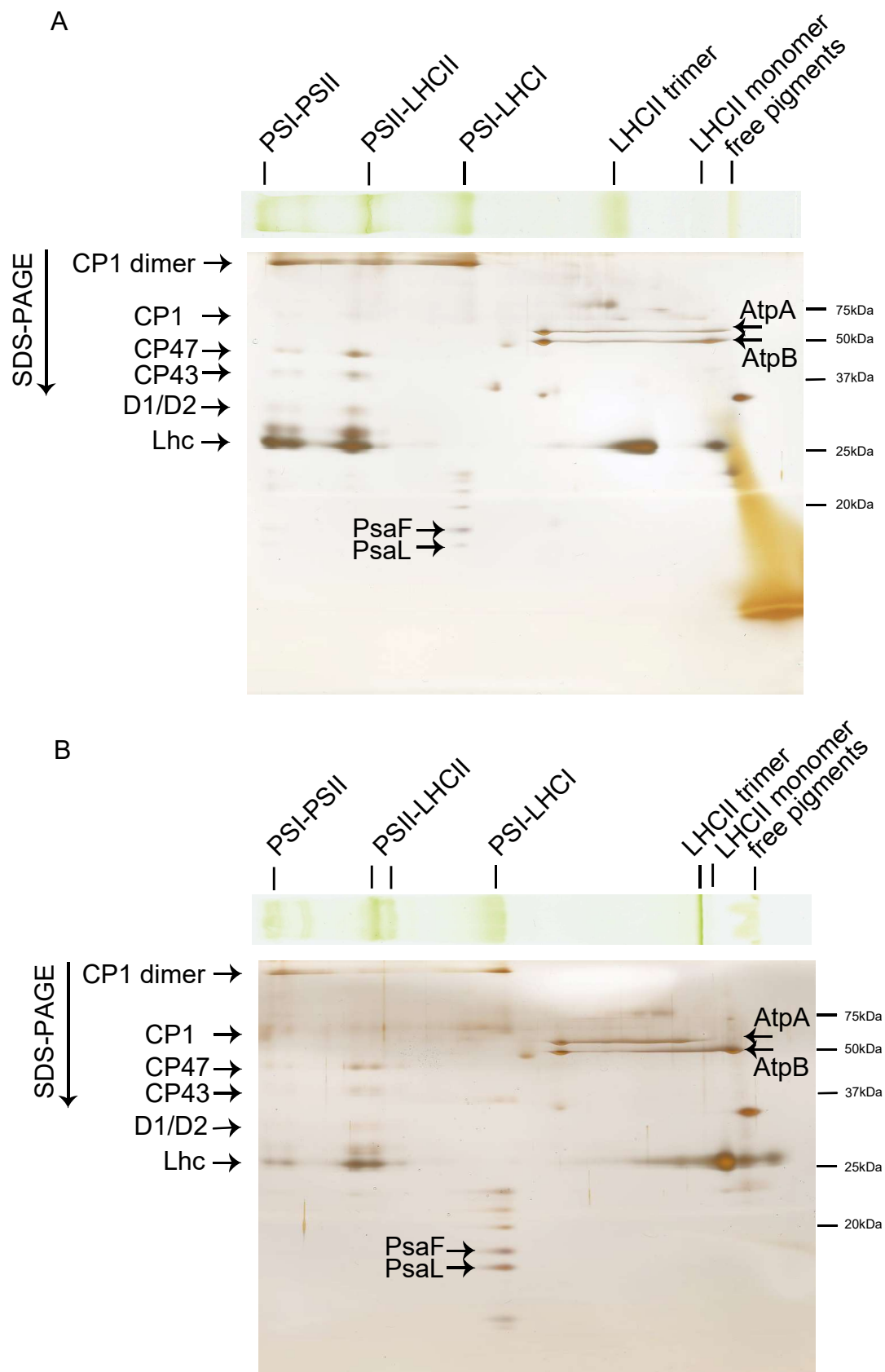


Fig. S2 2D-CN/SDS-PAGE followed by silver staining using the amphipol-based and DOC-based CN-PAGE gel strips for separation of *Physcomitrella* protein complexes in thylakoid membranes. The amphipol-based (A) and DOC-based (B) CN-PAGE gel strips (Fig. 6; upper) were soaked in 1% SDS and 50 mM DTT solution for 30 min. Proteins in the gel strips were resolved by SDS-PAGE using a 14% acrylamide gel containing 4 M urea and were visualized by silver staining.

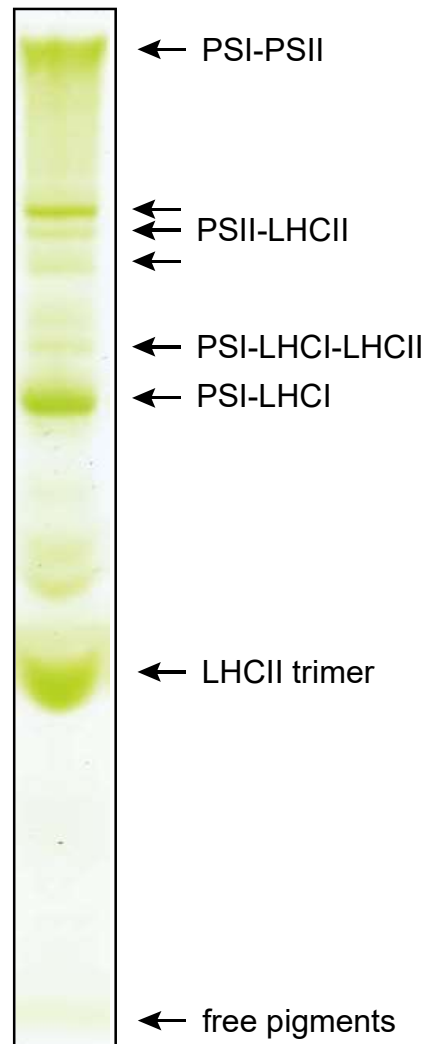


Fig. S3 Amphipol-based CN-PAGE of *Arabidopsis* protein complexes in thylakoid membranes solubilized by digitonin. *Arabidopsis* protein complexes in thylakoid membranes were solubilized by 1% digitonin and resolved by amphipol-based CN-PAGE using 4-13% acrylamide gels.